

Closed-form discovery of structural errors in models of chaotic systems by integrating Bayesian sparse regression and data assimilation

Rambod Mojtani,* Ashesh Chattopadhyay, and Pedram Hassanzadeh†

Rice University, Houston, TX 77005, USA

(Dated: October 4, 2021)

Models used for many important engineering and natural systems are imperfect. The discrepancy between the mathematical representations of a true physical system and its imperfect model is called the model error. These model errors can lead to substantial difference between the numerical solutions of the model and the observations of the system, particularly in those involving nonlinear, multi-scale phenomena. Thus, there is substantial interest in reducing model errors, particularly through understanding their physics and sources and leveraging the rapid growth of observational data. Here we introduce a framework named MEDIDA: Model Error Discovery with Interpretability and Data Assimilation. MEDIDA only requires a working numerical solver of the model and a small number of noise-free or noisy sporadic observations of the system. In MEDIDA, first the model error is estimated from differences between the observed states and model-predicted states (the latter are obtained from a number of one-time-step numerical integrations from the previous observed states). If observations are noisy, a data assimilation (DA) technique such as ensemble Kalman filter (EnKF) is first used to provide a noise-free analysis state of the system, which is then used in estimating the model error. Finally, an equation-discovery technique, such as the relevance vector machine (RVM), a sparsity-promoting Bayesian method, is used to identify an interpretable, parsimonious, closed-form representation of the model error. Using the chaotic Kuramoto-Sivashinsky (KS) system as the test case, we demonstrate the excellent performance of MEDIDA in discovering different types of structural/parametric model errors, representing different types of missing physics, using noise-free and noisy observations.

Keywords: model error, structural error, equation discovery, Bayesian machine learning, data assimilation, ensemble Kalman filter

I. INTRODUCTION

The discovery of the governing equations of physical systems is often based on the first principles, which has been the origin of most advances in science and engineering. However, in many important applications, some of the underlying physical processes are still not well understood, and therefore, are not included or are poorly represented in the mathematical (and thus numerical) models of these systems. Accordingly, these *imperfect models* (“models” hereafter) can merely closely track the dynamics of the *true physical system* (“system” hereafter), while failing to exactly represent it.

The difference between the solution of the model and the system becomes prominent in many problems involving complex, nonlinear, multi-scale phenomena such as those in engineering [1, 2, 3], thermo-fluids [4, 5], and climate/weather prediction [6, 7]; see Levine and Stuart [8] for an insightful overview. The deviation of the model from the system is called, in different communities, model uncertainty (structural and/or parametric), model discrepancy, model inadequacy, missing dynamics, or “model error”; hereafter, we will use the latter.

Recently, many studies have focused on leveraging the rapid advances in machine learning (ML) techniques and availability of data (e.g., high-quality observations) to

develop more accurate models. Several main approaches that best fit different applications have been pursued, including learning fully data-driven (equation-free) models [e.g., 9, 10, 11, 12, 13, 14, 15] or data-driven subgrid-scale closures [e.g., 16, 17, 18, 19, 20, 21, 22, 23, 24]. In a third approach, which is most directly focused on reducing the model error, corrections to the state or its temporal derivative (tendency) are learned from deviation of the model predictions from the observations [25, 26, 27, 28, 29]. More specifically, the model is initialized with the observed state, integrated forward in time, and the difference between the predicted state and the observation at the later time is computed. Repeated many times, a correction scheme, e.g., a deep neural network (DNN), can be trained to nudge the model’s predicted trajectory (or tendency) to that of the system every time. To deal with observations with measurement noise, particularly in the third approach, a number of studies have integrated data assimilation (DA) with DNNs [30, 31, 32, 33, 34, 35].

The above studies, which have shown promising results for a variety of test cases, often used DNNs. While powerfully expressive, DNNs are currently very hard to interpret and often fail to generalize (especially extrapolate) when the systems’ parameters change [e.g., 17, 24, 36, 37]. The interpretability of models is crucial for robust, reliable, and generalizable decision-critical predictions or designs [2, 7]. Posing the task of system identification as a linear regression problem, based on a library of nonlinear terms, exchanges the expressivity

* rm99@rice.edu

† pedram@rice.edu

of DNNs for the sake of interpretability [38, 39]. The closed-form representation of the identified models and their parsimony (i.e., sparsity in the space of the employed library) are the key advantages of these sparsity-promoting regression methods, leading to highly interpretable models. A number of studies have used such methods to discover closed-form full models or subgrid-scale closures [39, 40, 41, 42, 43, 44, 45]. While the results are promising, noisy data, especially in the chaotic regimes, can significantly degrade the quality of the discovered models [39, 42, 44, 45].

So far, there has not been any work on discovering closed-form representation of model error using the differences between model predictions and observations (approach 3) or on integrating the sparsity-promoting regression methods with DA to alleviate observation noise. Here, we introduce *MEDIDA* (Model Error Discovery with Interpretability and Data Assimilation). *MEDIDA* is a general-purpose, data-efficient, non-intrusive framework for discovering the structural (and parametric) model error in the form of missing/incorrect terms of partial differential equations (PDEs). *MEDIDA* uses differences between predictions from a working numerical solver of the model and noise-free or noisy sporadic observations. The framework is built on two main ideas:

- i) Discovering an interpretable and closed-form model error using relevance vector machine (RVM), a sparsity-promoting Bayesian regression method [46],
- ii) Alleviating the effects of measurement noise using DA methods such as ensemble Kalman filter (EnKF) to generate a noise-free “analysis state” from observations for (i).

After presenting the problem statement in §II, the key components of *MEDIDA* are described in §III. Then we demonstrate the performance of *MEDIDA* using the Kuramoto-Sivashinsky (KS) equation in the chaotic regime (§IV). Summary and discussions of prospective applications are in §V.

II. PROBLEM STATEMENT

Suppose that the exact mathematical representation of a physical system is a nonlinear PDE,

$$\partial_t u(t) = g(u(t)), \quad (1)$$

in a continuous domain with appropriate boundary conditions. Here, $u(t)$ is the state variable at time t . While (1) is not known, we assume to have access to sporadic (sparse in time) pairs of observations of the state variable u^o , though these observations might be contaminated by measurement noise. The set of observed states at t_i is denoted as $\{u^o(t_i - \Delta t), u^o(t_i)\}_{i=1}^n$. Note that t_i do not have to be equally spaced. Furthermore, Δt_i should be

similar for all i but do not have to be the same (hereafter, we use $\forall i, \Delta t_i = \Delta t$ for convenience).

Moreover, suppose that we have a *model* of the system,

$$\partial_t u(t) = f(u(t)). \quad (2)$$

Without loss of generality [8], we assume that the deviation of the model (2) from the system (1) is additive; we further assume that the deviation is only a function of the state [30, 31]. Therefore, the model error is

$$h(u(t)) := g(u(t)) - f(u(t)). \quad (3)$$

Our goal is to find a closed-form representation of the model error h given a working numerical solver of (2) and noisy or noise-free observations $\{u^o(t_i - \Delta t), u^o(t_i)\}_{i=1}^n$.

III. FRAMEWORK: MEDIDA

MEDIDA has three main steps (Fig. 1): Step 1) Collecting sporadic observations of the system and computing short-time evolutions of the model via numerical integration (§III A); Step 2) Construction of a regression problem, which is solved using RVM [46], leading to the sparse identification of the model error (§III B); Step 3) If observations are noisy, after Step 1, stochastic EnKF [47, 48] is used to estimate an analysis state, a noise-free estimate of the system’s state, for Step 2 (§III C). We emphasize that at no point in this framework we need any knowledge of the system (1). Also, note that other equation-discovery techniques and ensemble-based DA methods can be used in Steps 2-3.

A. Interpretable model error

Consider the discretized (2),

$$\mathbf{u}^m(t_i) = \mathbf{f}(\mathbf{u}^o(t_i - \Delta t)), \quad (4)$$

where for brevity, we have used the notation of an explicit scheme, but the scheme could be implicit too, as shown in the test case. The domain is discretized on the grid of $\mathbf{x} \in \mathbb{R}^M$. The observation at $t_i - \Delta t$, i.e., $\mathbf{u}^o(t_i - \Delta t)$, is the initial condition and $\mathbf{u}^m(t_i)$ is the predicted state at time t_i (Fig. 1a).

At each time t_i , subtracting the state predicted by the model ($\mathbf{u}^m(t_i)$) from the observed state ($\mathbf{u}^o(t_i)$) results in an approximation of the model error at t_i (Fig. 1b):

$$\mathbf{h}(t_i) \approx \Delta \mathbf{u}_i := (\mathbf{u}^o(t_i) - \mathbf{u}^m(t_i)) / \Delta t. \quad (5)$$

Note that for *MEDIDA* to accurately discover h as defined in (3), $\Delta \mathbf{u}_i$ should be *dominated by the model error*, and the contributions from numerical errors (in obtaining $\mathbf{u}^m(t_i)$) and measurement errors (in $\mathbf{u}^o(t_i)$) should be minimized as much as possible. Computing $\Delta \mathbf{u}_i$ after only one Δt prevents numerical error accumulation. While the size of Δt could be restricted by availability

of the observation pairs, increasing M can be used to reduce truncation errors from spatial discretizations. As discussed later, DA can be utilized to reduce the contributions from the measurement noise.

Integrating (4) from $\mathbf{u}^o(t_i - \Delta t)$ and computing $\Delta \mathbf{u}_i$ from (5) are repeated for all n samples (Step 1), and the vectors of model error are stacked to form $\Delta \mathbf{u} \in \mathbb{R}^{nM}$ (Step 2); see Fig. 1a-b. Similar to past studies [39, 40, 42, 49], we further assume that the model error spans over the space of the bases or training vectors, i.e.,

$$h(u(t)) = c_1 \phi_1 + \cdots + c_q \phi_q, \quad (6)$$

where ϕ_i is a linear or nonlinear function of the state variable, the building block of the library of training bases $\{\phi_k(u(t))\}_{k=1}^q$. Selection of these bases should be guided by the physical understanding of the system and the model.

Here, in the discretized form, we assume that $\Phi(\mathbf{u})$, also known as the design matrix, is a linear combination of polynomial terms up to p^{th} -order and spatial derivatives up to d^{th} -order, i.e.,

$$\Phi_k(\mathbf{u}) = \mathbf{u}^r \odot \mathbf{D}_x^s \mathbf{u} | r \in \mathbb{Z}^p, s \in \mathbb{Z}^d. \quad (7)$$

In (7), \mathbf{u}^r raises each element of \mathbf{u} to the power of r , $\mathbf{D}_x^s \mathbf{u}$ denotes the s^{th} spatial derivative of \mathbf{u} , and \odot is the element-wise (Hadamard) product. Therefore, the model error lies on the space of library of the training bases evaluated using the observed state at each t_i , $\Phi(\mathbf{u}^o, t_i) \in \mathbb{R}^{M \times q}$. For all the n samples, the vector library of the bases are stacked to form $\Phi(\mathbf{u}^o) \in \mathbb{R}^{nM \times q}$ (Fig. 1b).

At the end of Step 2, the regression problem for discovery of model error is formulated as

$$\mathbf{c}^* = \underset{\mathbf{c}}{\operatorname{argmin}} \|\Delta \mathbf{u} - \Phi(\mathbf{u}^o) \mathbf{c}\|_2, \quad (8)$$

where $\mathbf{c} \in \mathbb{R}^q$ is the vector of coefficients corresponding to the training bases, and $\mathbf{c}^* = [c_1^*, c_2^*, \dots, c_q^*]^\top$ is a minimizer of the regression problem, i.e., the vector of coefficients of the model error. Finally, the discovered (corrected) model is identified as

$$\partial_t u(t) = f(u(t)) + \sum_{k=1}^q c_k^* \phi_k(u(t)). \quad (9)$$

B. Solution of the regression problem

In this study, we use RVM [46] to compute \mathbf{c}^* in (8) for inputs of $\Delta \mathbf{u}$ and $\Phi(\mathbf{u}^o)$. RVMs lead to a sparse identification of columns of Φ with posterior distribution of the corresponding weights, i.e., the *relevant vectors*. See Zhang and Lin [40] for a detailed discussion of RVMs in the context of the discovery of PDEs.

The breakthrough in equation-discovery originates in introduction of parsimony [38]. While the original LASSO-type regularization has yielded promising results in a broad range of applications, RVMs have been found to achieve the desired sparsity by a more straightforward

hyper-parameter tuning and a relatively lower sensitivity to noise [40, 43, 50]. The hyper-parameter in RVMs is a threshold to prune the bases with higher posterior variance, i.e., highly uncertain bases are removed. We choose this hyper-parameter as a compromise between the sparsity and accuracy of the corrected model at the elbow of the L-curve, following Mangan et al. [51].

C. Data assimilation

The procedure described in §III A and §III B is enough to accurately find the corrected model (9) if observations are noise-free. However, noise can cause substantial challenges in the sparse identification of nonlinear systems, a topic that is the subject of ongoing research [39, 41, 42, 50, 52].

In MEDIDA, we propose to use DA, a powerful set of tools to deal with noisy observations. Here, we use stochastic EnKF [53]; see (Fig. 1c. Briefly, for sample i , $\mathbf{u}^o(t_i - \Delta t)$ and $\mathbf{u}^o(t_i)$ are perturbed, respectively, with $\mathcal{N}(0, \sigma_b^2)$ and $\mathcal{N}(0, \sigma_{obs}^2)$ to generate an ensemble of N members for each; σ_{obs} is the standard deviation of the observation noise, σ_b is σ_{obs} times an inflation factor [47, 54]. Then (4) is integrated from each ensemble member $\mathbf{u}_k^o(t_i - \Delta t)$ to predict $\mathbf{u}_k^m(t_i)$. The N -member ensembles of $\mathbf{u}_k^m(t_i)$ and $\mathbf{u}_k^o(t_i)$ are then used to compute the analysis state $\mathbf{u}_k^a(t_i)$; see Fig. 1c for the equations. The ensemble-mean of the latter, $\overline{\mathbf{u}}^a(t_i)$, computed for all n samples, is used as a noise-free estimate of the system's state in place of noisy \mathbf{u}^o in (5) and (7)-(8).

D. Performance metric

To quantify the accuracy of MEDIDA, we use the normalized distance between the coefficients of the terms in the system and in the original or corrected model, computed, respectively, as [39, 42]

$$\varepsilon_m = \frac{\|\mathbf{c}_s - \mathbf{c}_m\|_2}{\|\mathbf{c}_s\|_2} \quad \text{and} \quad \varepsilon^* = \frac{\|\mathbf{c}_s - \mathbf{c}^*\|_2}{\|\mathbf{c}_s\|_2}. \quad (10)$$

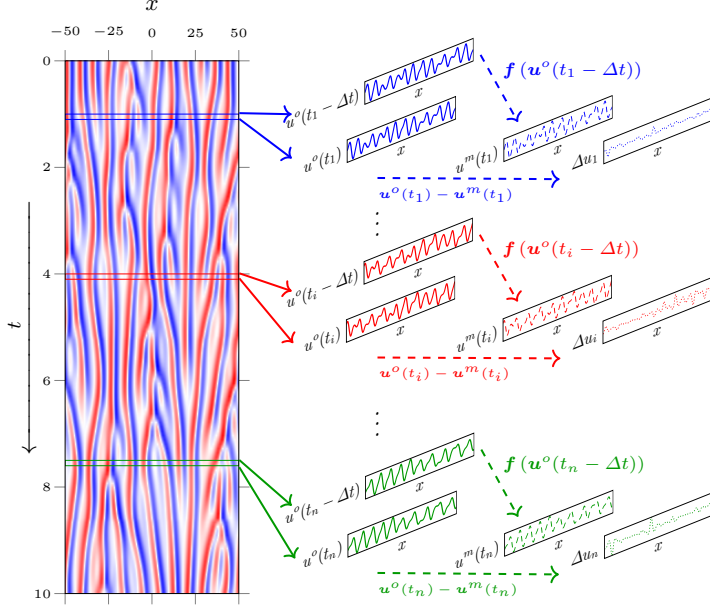
Here, \mathbf{c}_s is a vector of the coefficients of the terms in the system (1). \mathbf{c}_m and \mathbf{c}^* are, respectively, the vector of coefficients in the original (2) and corrected (9) models. Quantitatively, the goal of MEDIDA is to achieve $\varepsilon^* \ll \varepsilon_m$.

IV. TEST CASE: KS EQUATION

To evaluate the performance of MEDIDA, we use the KS equation in the chaotic regime, which has been found a challenging test case for system identification, particularly in the presence of observation noise [39, 42]. The PDE is

$$\partial_t u + u \partial_x u + \partial_x^2 u + \partial_x^4 u = 0, \quad (11)$$

(a) Step 1: Observation and model prediction



(b) Step 2: Forming the regression problem

$$\Delta \mathbf{u} = \begin{bmatrix} \frac{1}{\Delta t} (\mathbf{u}^o(t_1) - \mathbf{u}^m(t_1)) \\ \vdots \\ \frac{1}{\Delta t} (\mathbf{u}^o(t_i) - \mathbf{u}^m(t_i)) \\ \vdots \\ \frac{1}{\Delta t} (\mathbf{u}^o(t_n) - \mathbf{u}^m(t_n)) \end{bmatrix}$$

$$\Phi(\mathbf{u}^o) = \begin{bmatrix} \Phi_1 & \Phi_2 & \Phi_3 & \dots & \Phi_q \\ \mathbf{1} & \mathbf{u}^{o1}(t_1) & \mathbf{u}^{o2}(t_1) & \dots & \mathbf{u}^{op}(t_1) \odot \mathbf{D}_x^d \mathbf{u}(t_1) \\ \vdots & \vdots & \vdots & \ddots & \vdots \\ \mathbf{1} & \mathbf{u}^{o1}(t_i) & \mathbf{u}^{o2}(t_i) & \dots & \mathbf{u}^{op}(t_i) \odot \mathbf{D}_x^d \mathbf{u}(t_i) \\ \vdots & \vdots & \vdots & \ddots & \vdots \\ \mathbf{1} & \mathbf{u}^{o1}(t_n) & \mathbf{u}^{o2}(t_n) & \dots & \mathbf{u}^{op}(t_n) \odot \mathbf{D}_x^d \mathbf{u}(t_n) \end{bmatrix}$$

$\Delta \mathbf{u}$ and $\Phi(\mathbf{u}^o)$ are fed into (8)

(c) Step 3: EnKF is used to assimilate noisy observations for Step 2

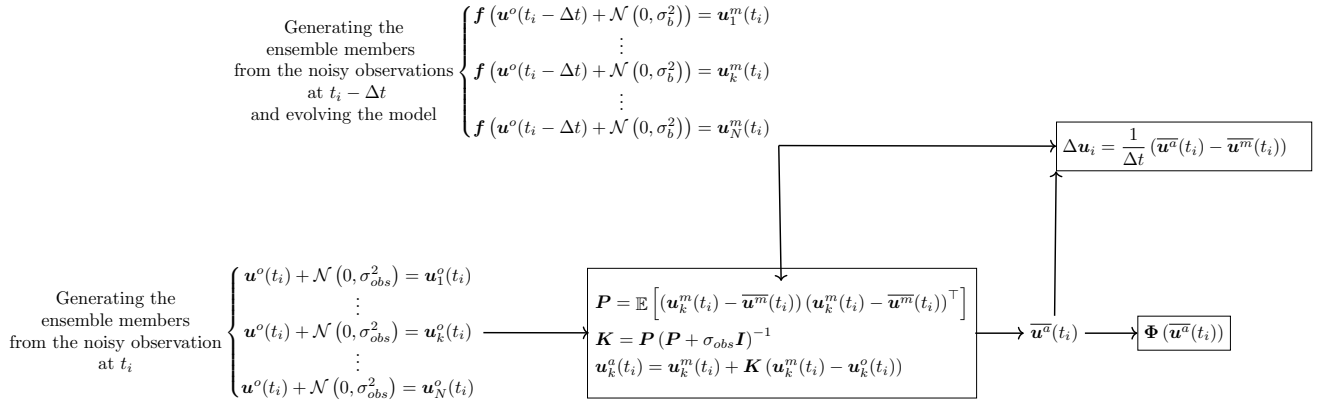


FIG. 1. The schematic of MEDIDA, presented in the context of the test case in §IV. (a) Step 1: n pairs of state variables are sampled uniformly or non-uniformly at t_i from observations (of the system (1)) to obtain $\{\mathbf{u}^o(t_i - \Delta t), \mathbf{u}^o(t_i)\}_{i=1}^n$. The model (4) is integrated numerically for one time-step from each $\mathbf{u}^o(t_i - \Delta t)$ to predict $\mathbf{u}^m(t_i)$. For each sample, at t_i , the difference between the predicted and observed state is used to compute $\Delta \mathbf{u}_i$ (5), an approximation of model error. (b) Step 2: $\{\Delta \mathbf{u}_i\}_{i=1}^n$ are stacked to form $\Delta \mathbf{u}$. Moreover, the library of bases $\Phi(\mathbf{u}^o)$, consisting of selected q linear and nonlinear bases evaluated at $\{\mathbf{u}^o(t_i)\}_{i=1}^n$, is formed. Here, the library in (7) is used, but the bases with any arbitrary functional form could be used depending on the anticipated form of the model error. $\Delta \mathbf{u}$ and Φ are then fed into the RVM (or other equation-discovery methods) to compute \mathbf{c}^* for minimizing the loss function (8). The corrected model is then identified using \mathbf{c}^* as Eq. (9). (c) Step 3: If observations are noisy, DA is used to provide an “analysis state” $\{\mathbf{u}^a(t_i)\}_{i=1}^n$, a noise-free estimate of the system’s state, to be used in place of $\{\mathbf{u}^o(t_i)\}_{i=1}^n$ for computing $\Delta \mathbf{u}$ and Φ in Steps 1-2. Here we use a stochastic EnKF for DA: For each sample i , the noisy observation is perturbed by Gaussian white noise with inflated standard deviation σ_b to generate an ensemble of size N . Each ensemble member k is numerically evolved by the model, $\{\mathbf{f}(\mathbf{u}_k^o(t_i - \Delta t))\}_{k=1}^N$, to generate the ensemble of model prediction $\{\mathbf{u}_k^m(t_i)\}_{k=1}^N$. Observations at time t_i are also perturbed by Gaussian white noise with standard deviation σ_{obs} to generate the ensemble $\{\mathbf{u}_k^o(t_i)\}_{k=1}^N$. These two ensembles are then used to compute the background covariance matrix \mathbf{P} , Kalman gain \mathbf{K} , and finally, the analysis state $\bar{\mathbf{u}}^a(t_i)$; overbars indicate ensemble mean and $\mathbb{E}[\cdot]$ denotes expectation. $\Delta \mathbf{u}$ and Φ in Steps 1-2 are then computed using $\bar{\mathbf{u}}^a(t_i)$.

in which $u \partial_x u$ is nonlinear convection, $\partial_x^2 u$ is anti-diffusion (thus destabilizing), and $\partial_x^4 u$ is hyper-diffusion

(thus stabilizing). This combination leads to small-scale

dissipations and large-scale instabilities, transferring energy from the large to small scales [55, 56]. The domain is periodic, $u(0, t) = u(L, t)$, where L , the domain length, determines the dimension of the attractor [57]; larger L is expected to increase the complexity of the model error discovery. We set $L = 32\pi$, which leads to a highly chaotic system [9, 58].

Here, (11) is the system. We have created 9 (imperfect) models for (11), Cases 1-9 in Tables I-II. In Cases 1-3, the nonlinear convection, anti-diffusion, or hyperdiffusion term is entirely missing (i.e., structural uncertainty). In Cases 4-6, some or all of the coefficients of the system are incorrect (i.e., parameter uncertainty). Finally, in Cases 7-9, a mixture of parameter and structural uncertainties, with missing and extra terms, is present.

The system (11) and the models are numerically solved using different time-integration schemes and time-step sizes to introduce additional challenges and a more realistic test case. To generate \mathbf{u}^o , (11) is integrated with the exponential time-differencing fourth-order Runge-Kutta [59] with time-step Δt^o (in Fig. 1a, $1t = 10^3 \Delta t^o$). The models are integrated with second-order Crank-Nicolson and Adams-Bashforth schemes with $\Delta t^m = \Delta t = 5\Delta t^o$. For both system and models, $M = 1024$ Fourier modes are used (different discretizations or M for system and models could have been used too). \mathbf{u}^o is collected after a spin-up period of $\tau = 200\Delta t$ and uniformly at $t_i = i\tau$. The library of bases, Φ , is constructed with $d = 4$ and $p = 4$ as defined in (7). We have used open-source codes to generate the library of the bases [39] and solve (8) using RVM [43].

A. Noise-free observations

First, we examine the performance of MEDIDA for noise-free observations (only Steps 1-2). The motivation is two-fold: i) it provides a test bench for Steps 1-2 before adding the complexity of noisy observations and DA, and ii) in many important applications, a noise-free estimate of \mathbf{u}^o is already available (see §V).

In this test case, \mathbf{u}^o are from the numerical solutions of the system (11). The models, MEDIDA-corrected models, and the corresponding errors for $n = 100$ samples are summarized in Table I. In all cases, the corrected models are very close to the system, with $\varepsilon^* < 2\%$ and between 40 to 200 times lower than ε_m .

MEDIDA is a data-efficient framework. In these cases, its performance is insensitive to n , such that ε^* changes by 0.1% for $n \in \{10, 100, 1000\}$. There are two reasons for this: first, RVM is known to be data-efficient (compared to DNNs) [60], and second, in MEDIDA, each grid point at t_i provides a data-point, i.e., a row in $\Delta \mathbf{u}$ and Φ , although these are not all independent/uncorrelated data-points.

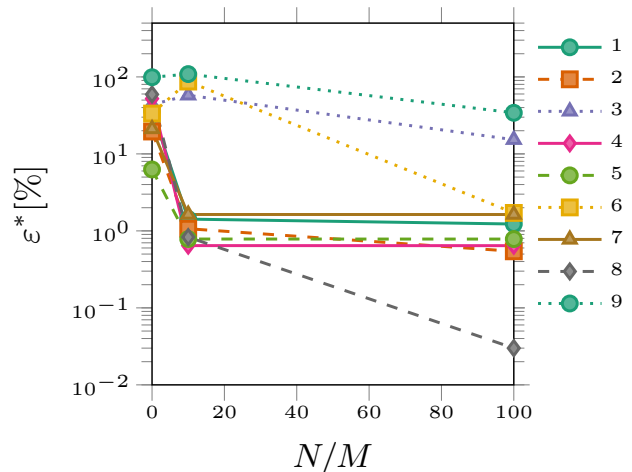


FIG. 2. Improvement in the performance of MEDIDA as the ensemble size, N , is increased ($n = 100$). $N/M = 0$ corresponds to no DA. ε^* for Cases 3 and 9 further drops to 0.98% and 0.55% using larger ensembles with $N = 200M$ and $N = 500M$, respectively (Table II).

B. Noisy observations

Next, we examine the performance of MEDIDA for noisy observations, obtained from adding noise to the numerical solution of the system (11):

$$\mathbf{u}^o(t) = \mathbf{u}(t) + \mathcal{N}(0, \sigma_{obs}^2). \quad (12)$$

Here, $\sigma_{obs}/\sigma_u = 0.01$, where σ_u is the standard deviation of the solution of (11). Without Step 3 (DA), the model error discovery fails, leading to many spurious terms and ε^* of $O(10\%) - O(100\%)$, comparable or even worse than ε_m (Fig. 2).

Table II shows the MEDIDA-corrected models (with Step 1-3). With $N = 10M$, in all cases except for 3, 6, and 9, $\varepsilon^* < 2\%$ and between 30 to 60 times lower than ε_m . For those 3 cases, increasing N further reduces ε^* (Fig. 2), leading to the discovery of accurate models with $\varepsilon^* < 1\%$ at large ensembles with $N = 100M - 500M$ (Table II). Note that one common aspect of these 3 cases is that the model is missing or mis-representing the hyperdiffusion term. The larger N is needed to further reduce the noise in the analysis state to prevent amplification of the noise due to the higher-order derivative of this term. It should also be highlighted that while N at the order of M or larger might seem impractical, each ensemble member requires only *one* time-step integration (thus, a total of nN time steps).

MEDIDA is found to be data-efficient in these experiments too. Like before, ε^* changes by 0.1% for $n \in \{10, 100, 1000\}$ for all cases except for 3, 6, and 9. For these 3 cases, ε^* improves by about 10% as n is increased from 10 to 100, but then changes by only 0.1% when n is further increased to 1000.

TABLE I. MEDIDA-corrected models from noise-free observations of the system for the 9 cases. ε_m and ε^* are defined in (10).

System: $\partial_t u + u\partial_x u + \partial_x^2 u + \partial_x^4 u = 0$				
#	Model: $0 = \partial_t u +$	ε_m [%]	Corrected model: $0 = \partial_t u +$	ε^* [%]
1	$\partial_x^2 u + \partial_x^4 u$	57.74	$0.97u\partial_x u + \partial_x^2 u + \partial_x^4 u$	1.50
2	$u\partial_x u + \partial_x^4 u$	57.74	$u\partial_x u + 0.99\partial_x^2 u + \partial_x^4 u$	0.39
3	$u\partial_x u + \partial_x^2 u$	57.74	$u\partial_x u + \partial_x^2 u + 1.02\partial_x^4 u$	1.08
4	$0.5u\partial_x u + \partial_x^2 u + \partial_x^4 u$	28.87	$0.99u\partial_x u + \partial_x^2 u + \partial_x^4 u$	0.75
5	$u\partial_x u + 0.5\partial_x^2 u + \partial_x^4 u$	28.87	$u\partial_x u + 1.00\partial_x^2 u + \partial_x^4 u$	0.14
6	$u\partial_x u + \partial_x^2 u + 0.5\partial_x^4 u$	28.87	$u\partial_x u + \partial_x^2 u + 1.00\partial_x^4 u$	0.14
7	$0.5u\partial_x u + 2\partial_x^4 u$	86.60	$0.97u\partial_x u + 1.00\partial_x^2 u + \partial_x^4 u$	1.55
8	$u\partial_x u + \partial_x^2 u + 0.5\partial_x^3 u + \partial_x^4 u$	28.87	$u\partial_x u + \partial_x^2 u + \partial_x^4 u$	0.28
9	$u\partial_x u + \partial_x^2 u + 0.5\partial_x^3 u$	64.55	$u\partial_x u + \partial_x^2 u - 0.01\partial_x^3 u + 1.02\partial_x^4 u$	1.29

TABLE II. MEDIDA-corrected models from noisy observations of the system ($\sigma_{obs}/\sigma_u = 0.01$) for the 9 cases. ε_m and ε^* are defined in (10). For all cases, $\sigma_b = 20\sigma_{obs}$ is used. The ensemble size is $N = 10M$ for all cases, except for 6^\dagger with $N = 100M$, 3^\ddagger with $N = 200M$, and $9^{\dagger\dagger}$ with $N = 500M$.

System: $\partial_t u + u\partial_x u + \partial_x^2 u + \partial_x^4 u = 0$				
#	Model: $0 = \partial_t u +$	ε_m [%]	Corrected model: $0 = \partial_t u +$	ε^* [%]
1	$\partial_x^2 u + \partial_x^4 u$	57.74	$0.98u\partial_x u + \partial_x^2 u + \partial_x^4 u$	1.43
2	$u\partial_x u + \partial_x^4 u$	57.74	$u\partial_x u + 0.98\partial_x^2 u + \partial_x^4 u$	0.98
3^\ddagger	$u\partial_x u + \partial_x^2 u$	57.74	$u\partial_x u + \partial_x^2 u + 1.02\partial_x^4 u$	0.98
4	$0.5u\partial_x u + \partial_x^2 u + \partial_x^4 u$	28.87	$0.99u\partial_x u + \partial_x^2 u + \partial_x^4 u$	0.63
5	$u\partial_x u + 0.5\partial_x^2 u + \partial_x^4 u$	28.87	$u\partial_x u + 0.98\partial_x^2 u + \partial_x^4 u$	0.99
6^\dagger	$u\partial_x u + \partial_x^2 u + 0.5\partial_x^4 u$	28.87	$u\partial_x u + \partial_x^2 u + 1.00\partial_x^4 u$	0.15
7	$0.5u\partial_x u + 2\partial_x^4 u$	86.60	$0.98u\partial_x u + 0.98\partial_x^2 u + \partial_x^4 u$	1.63
8	$u\partial_x u + \partial_x^2 u + 0.5\partial_x^3 u + \partial_x^4 u$	28.87	$u\partial_x u + \partial_x^2 u - 0.01\partial_x^3 u + \partial_x^4 u$	0.83
$9^{\dagger\dagger}$	$u\partial_x u + \partial_x^2 u + 0.5\partial_x^3 u$	64.55	$u\partial_x u + \partial_x^2 u - 0.01\partial_x^3 u + 1.00\partial_x^4 u$	0.55

V. DISCUSSION AND SUMMARY

We introduced MEDIDA which is a data-efficient, non-intrusive framework to discover interpretable, closed-form structural (or parametric) model error for chaotic systems. MEDIDA only needs a working numerical solver of the model and n sporadic pairs of noise-free or noisy observations of the system. Model error is estimated from differences between the observed states and predicted states (obtained from one-time-step integrations of the model from earlier observed states as initial conditions). A closed-form representation of the estimated model error is obtained using an equation-discovery technique such as RVM. MEDIDA is expected to work accurately i) if the aforementioned differences are dominated by model error and not by numerical (discretization) error or observation noise, and ii) if the library used in the RVM is adequate (further discussed below). As for (i), the numerical error can be reduced using higher numerical resolutions while the observation noise can be tackled using DA techniques such as EnKF.

The performance of MEDIDA is demonstrated using

a chaotic KS system for both noise-free and noisy observations. In the absence of noise, even with a small n , MEDIDA shows excellent performance and accurately discovers linear and nonlinear model errors, leading to corrected models that are very close to the system. These results already show the potential of MEDIDA as in some important applications, noise-free estimates of the system (analysis states) are routinely generated and are available; this is often the case for atmosphere and some other components of the Earth system. For example, such analysis states have been recently used by Watt-Meyer et al. [29] to correct the model error of a numerical weather prediction model using a DNN.

In the presence of noise, the model error could not be accurately discovered without DA. Once EnKF is employed, MEDIDA again accurately discovers linear and nonlinear model errors. A few cases in which the model error involves linear but 4th-order derivatives require larger ensemble sizes. This is because higher-quality analysis states are needed to avoid amplification of any remaining noise as a result of high-order derivatives. As mentioned in §IV B, producing a large ensemble

is not necessarily computationally demanding here, because each member only requires one time-step integration. Still, if needed, inexpensive surrogates of the model that could provide accurate one-time-step forecasts can be used to efficiently produce a large ensemble [35].

Also, it should be highlighted that in EnKF, ensemble members are evolved using the model. If model error is large, the computed analysis state might be too far from the system’s state, degrading the performance of MEDIDA. In all cases that are examined here, even though the model errors are large, with large-enough ensembles, the analysis states are accurate enough to enable MEDIDA to perform well. However, in more complex systems, this might become a challenge that requires devising new remedies. One potential resolution is an iterative procedure, in which the analysis state is generated and a corrected model is identified, which is then used to produce a new analysis state and a new corrected model, and this continues until convergence. The cost and possible convergence issues of such an approach remain to be investigated in more complex test cases. Note that other ideas for dealing with observation noise in equation discovery [e.g., 42, 61] could be also integrated with DA in MEDIDA.

As mentioned above, the choice of the library in RVM is important for the performance of MEDIDA. Building an exhaustive library of the training vectors and inclusion of any arbitrary nonlinearity and function is straightforward but becomes computationally intractable quickly. Any *a priori* knowledge of the system, such as locality, homogeneity [30], Galilean invariance, and most impor-

tantly conservation properties [40] can be considered to construct a more concise library. Conversely, the library can be expanded to systematically “explore the computational universe”, e.g., using gene expression programming [62]. Even further, additional constraints, for example on stability of the corrected model, can be imposed [63]. Effective strategies for the selection of an adequate and concise library should be investigated in future work using more complex test cases.

To summarize, MEDIDA is a novel, general-purpose framework for interpretable model error discovery and has shown promising performance, in terms of both accuracy and data efficiency, in a canonical chaotic test case. Application of MEDIDA to more complex test cases is currently underway.

ACKNOWLEDGMENTS

We thank Yifei Guan for helpful comments on the manuscript. This work was supported by an award from the ONR Young Investigator Program (N00014-20-1-2722), a grant from the NSF CSSI program (OAC-2005123), and by the generosity of Eric and Wendy Schmidt by recommendation of the Schmidt Futures program. Computational resources were provided by NSF XSEDE (allocation ATM170020) and NCAR’s CISL (allocation URIC0004). Our codes and data are available at <https://github.com/envfluids/MEDIDA>.

-
- [1] B. M. de Silva, D. M. Higdon, S. L. Brunton, J. N. Kutz, Discovery of physics from data: Universal laws and discrepancies, *Frontiers in Artificial Intelligence* 3 (2020) 1–17. [arXiv:1906.07906](https://arxiv.org/abs/1906.07906).
 - [2] K. E. Willcox, O. Ghattas, P. Heimbach, The imperative of physics-based modeling and inverse theory in computational science, *Nature Computational Science* 1 (2021) 166–168.
 - [3] F. Regazzoni, D. Chapelle, P. Moireau, Combining data assimilation and machine learning to build data-driven models for unknown long time dynamics—applications in cardiovascular modeling, *International Journal for Numerical Methods in Biomedical Engineering* 37 (2021) e3471.
 - [4] A. Subramanian, S. Mahadevan, Model error propagation in coupled multiphysics systems, *AIAA Journal* 58 (2020) 2236–2245.
 - [5] K. Duraisamy, Perspectives on machine learning-augmented Reynolds-averaged and large eddy simulation models of turbulence, *Physical Review Fluids* 6 (2021) 050504.
 - [6] V. Balaji, Climbing down Charney’s ladder: machine learning and the post-Dennard era of computational climate science, *Philosophical Transactions of the Royal Society A* 379 (2021) 20200085.
 - [7] T. Schneider, N. Jeevanjee, R. Socolow, Accelerating progress in climate science, *Physics Today* 74 (2021) 44–51.
 - [8] M. E. Levine, A. M. Stuart, A framework for machine learning of model error in dynamical systems, *arXiv preprint arXiv:2107.06658* (2021).
 - [9] J. Pathak, B. Hunt, M. Girvan, Z. Lu, E. Ott, Model-free prediction of large spatiotemporally chaotic systems from data: A reservoir computing approach, *Physical Review Letters* 120 (2018) 024102.
 - [10] P. R. Vlachas, W. Byeon, Z. Y. Wan, T. P. Sapsis, P. Koumoutsakos, Data-driven forecasting of high-dimensional chaotic systems with long short-term memory networks, *Proceedings of the Royal Society A: Mathematical, Physical and Engineering Sciences* 474 (2018) 20170844.
 - [11] P. D. Dueben, P. Bauer, Challenges and design choices for global weather and climate models based on machine learning, *Geoscientific Model Development* 11 (2018) 3999–4009.
 - [12] J. A. Weyn, D. R. Durran, R. Caruana, Can machines learn to predict weather? using deep learning to predict gridded 500-hpa geopotential height from historical weather data, *Journal of Advances in Modeling Earth Systems* 11 (2019) 2680–2693.
 - [13] A. Chattopadhyay, P. Hassanzadeh, D. Subramanian, Data-driven predictions of a multiscale Lorenz 96 chaotic

- system using machine-learning methods: reservoir computing, artificial neural network, and long short-term memory network, *Nonlinear Processes in Geophysics* 27 (2020) 373–389.
- [14] T. Arcomano, I. Szunyogh, J. Pathak, A. Wikner, B. R. Hunt, E. Ott, A machine learning-based global atmospheric forecast model, *Geophysical Research Letters* 47 (2020) e2020GL087776.
- [15] A. Chattopadhyay, E. Nabizadeh, P. Hassanzadeh, Analog forecasting of extreme-causing weather patterns using deep learning, *Journal of Advances in Modeling Earth Systems* 12 (2020) e2019MS001958.
- [16] C. Ma, J. Wang, W. E. Model reduction with memory and the machine learning of dynamical systems, *arXiv preprint arXiv:1808.04258* (2018). [arXiv:1808.04258](https://arxiv.org/abs/1808.04258).
- [17] S. Rasp, M. S. Pritchard, P. Gentine, Deep learning to represent subgrid processes in climate models, *Proceedings of the National Academy of Sciences* 115 (2018) 9684–9689.
- [18] R. Maulik, O. San, A. Rasheed, P. Vedula, Subgrid modelling for two-dimensional turbulence using neural networks, *Journal of Fluid Mechanics* 858 (2019) 122–144.
- [19] N. D. Brenowitz, C. S. Bretherton, Spatially extended tests of a neural network parametrization trained by coarse-graining, *Journal of Advances in Modeling Earth Systems* 11 (2019) 2728–2744.
- [20] T. Bolton, L. Zanna, Applications of deep learning to ocean data inference and subgrid parameterization, *Journal of Advances in Modeling Earth Systems* 11 (2019) 376–399.
- [21] A. Beck, D. Flad, C.-D. Munz, Deep neural networks for data-driven LES closure models, *Journal of Computational Physics* 398 (2019) 108910.
- [22] A. Subel, A. Chattopadhyay, Y. Guan, P. Hassanzadeh, Data-driven subgrid-scale modeling of forced Burgers turbulence using deep learning with generalization to higher Reynolds numbers via transfer learning, *Physics of Fluids* 33 (2021).
- [23] J. Harlim, S. W. Jiang, S. Liang, H. Yang, Machine learning for prediction with missing dynamics, *Journal of Computational Physics* 428 (2021) 109922.
- [24] Y. Guan, A. Chattopadhyay, A. Subel, P. Hassanzadeh, Stable a posteriori LES of 2D turbulence using convolutional neural networks: Backscattering analysis and generalization to higher Re via transfer learning, *arXiv preprint arXiv:2102.11400v1* (2021).
- [25] P. A. Watson, Applying machine learning to improve simulations of a chaotic dynamical system using empirical error correction, *Journal of Advances in Modeling Earth Systems* 11 (2019) 1402–1417.
- [26] S. Pawar, S. E. Ahmed, O. San, A. Rasheed, I. M. Navon, Long short-term memory embedded nudging schemes for nonlinear data assimilation of geophysical flows, *Physics of Fluids* 32 (2020) 076606.
- [27] J. Pathak, M. Mustafa, K. Kashinath, E. Motheau, T. Kurth, M. Day, Using machine learning to augment coarse-grid computational fluid dynamics simulations, *arXiv preprint arXiv:2010.00072* (2020).
- [28] C. S. Bretherton, B. Henn, A. Kwa, N. D. Brenowitz, O. Watt-Meyer, J. McGibbon, W. A. Perkins, S. K. Clark, L. Harris, Correcting coarse-grid weather and climate models by machine learning from global storm-resolving simulations, *Earth and Space Science Open Archive* (2021) 39.
- [29] O. Watt-Meyer, N. D. Brenowitz, S. K. Clark, B. Henn, A. Kwa, J. McGibbon, W. A. Perkins, C. S. Bretherton, Correcting weather and climate models by machine learning nudged historical simulations, *Geophysical Research Letters* 48 (2021) e2021GL092555.
- [30] M. Bocquet, J. Brajard, A. Carrassi, L. Bertino, Data assimilation as a learning tool to infer ordinary differential equation representations of dynamical models, *Nonlinear Processes in Geophysics* 26 (2019) 143–162.
- [31] A. Farchi, P. Laloyaux, M. Bonavita, M. Bocquet, Using machine learning to correct model error in data assimilation and forecast applications, *Quarterly Journal of the Royal Meteorological Society* (2021) qj.4116. [arXiv:2010.12605](https://arxiv.org/abs/2010.12605).
- [32] J. Brajard, A. Carrassi, M. Bocquet, L. Bertino, Combining data assimilation and machine learning to emulate a dynamical model from sparse and noisy observations: A case study with the Lorenz 96 model, *Journal of Computational Science* 44 (2020) 101171.
- [33] N. Chen, Y. Li, BAMCAFE: A Bayesian machine learning advanced forecast ensemble method for complex nonlinear turbulent systems with partial observations (2021). [arXiv:2107.05549](https://arxiv.org/abs/2107.05549).
- [34] A. Wikner, J. Pathak, B. R. Hunt, I. Szunyogh, M. Girvan, E. Ott, Using data assimilation to train a hybrid forecast system that combines machine-learning and knowledge-based components, *Chaos: An Interdisciplinary Journal of Nonlinear Science* 31 (2021) 053114.
- [35] A. Chattopadhyay, M. Mustafa, P. Hassanzadeh, E. Bach, K. Kashinath, Towards physically consistent data-driven weather forecasting: Integrating data assimilation with equivariance-preserving spatial transformers in a case study with ERA5, *Geoscientific Model Development Discussions* (2021) 1–23.
- [36] A. Chattopadhyay, A. Subel, P. Hassanzadeh, Data-driven super-parameterization using deep learning: Experimentation with multi-scale Lorenz 96 systems and transfer-learning, *Journal of Advances in Modeling Earth Systems* (2020) e2020MS002084.
- [37] R. Mojjani, M. Balajewicz, Low-rank registration based manifolds for convection-dominated PDEs, *Proceedings of the AAAI Conference on Artificial Intelligence* 35 (2021) 399–407.
- [38] S. L. Brunton, J. L. Proctor, J. N. Kutz, Discovering governing equations from data by sparse identification of nonlinear dynamical systems, *Proceedings of the national academy of sciences* 113 (2016) 3932–3937.
- [39] S. H. Rudy, S. L. Brunton, J. L. Proctor, J. N. Kutz, Data-driven discovery of partial differential equations, *Science Advances* 3 (2017) e1602614.
- [40] S. Zhang, G. Lin, Robust data-driven discovery of governing physical laws with error bars, *Proceedings of the Royal Society A: Mathematical, Physical and Engineering Sciences* 474 (2018) 20180305.
- [41] H. Schaeffer, G. Tran, R. Ward, Extracting sparse high-dimensional dynamics from limited data, *SIAM Journal on Applied Mathematics* 78 (2018) 3279–3295.
- [42] P. A. K. Reinbold, D. R. Gurevich, R. O. Grigoriev, Using noisy or incomplete data to discover models of spatiotemporal dynamics, *Physical Review E* 101 (2020) 010203(R). [arXiv:1911.03365](https://arxiv.org/abs/1911.03365).
- [43] L. Zanna, T. Bolton, Data-driven equation discovery of ocean mesoscale closures, *Geophysical Research Letters* 47 (2020) e2020GL088376.

- [44] D. A. Messenger, D. M. Bortz, Weak SINDy for partial differential equations, *Journal of Computational Physics* 443 (2021) 110525.
- [45] A. Cortiella, K. C. Park, A. Doostan, Sparse identification of nonlinear dynamical systems via reweighted l_1 -regularized least squares, *Computer Methods in Applied Mechanics and Engineering* 376 (2021) 113620. [arXiv:2005.13232](#).
- [46] M. E. Tipping, Sparse Bayesian learning and the relevance vector machine, *Journal of Machine Learning Research* 1 (2001) 211–244.
- [47] M. Asch, M. Bocquet, M. Nodet, *Data assimilation: methods, algorithms, and applications*, SIAM, 2016.
- [48] K. Law, A. Stuart, K. Zygalakis, *Data Assimilation: A Mathematical Introduction*, Texts in Applied Mathematics, Springer International Publishing, 2015.
- [49] S. Zhang, G. Lin, SubTSBR to tackle high noise and outliers for data-driven discovery of differential equations, *Journal of Computational Physics* 428 (2021) 109962.
- [50] S. H. Rudy, T. P. Sapsis, Sparse methods for automatic relevance determination, *Physica D: Nonlinear Phenomena* 418 (2021) 132843.
- [51] N. M. Mangan, J. N. Kutz, S. L. Brunton, J. L. Proctor, Model selection for dynamical systems via sparse regression and information criteria, *Proceedings of the Royal Society A: Mathematical, Physical and Engineering Sciences* 473 (2017) 20170009.
- [52] P. Goyal, P. Benner, Discovery of nonlinear dynamical systems using a Runge-Kutta inspired dictionary-based sparse regression approach, 2105.04869 (2021). [arXiv:2105.04869](#).
- [53] G. Evensen, Sequential data assimilation with a nonlinear quasi-geostrophic model using monte carlo methods to forecast error statistics, *Journal of Geophysical Research: Oceans* 99 (1994) 10143–10162.
- [54] J. L. Anderson, S. L. Anderson, A Monte Carlo implementation of the nonlinear filtering problem to produce ensemble assimilations and forecasts, *Monthly Weather Review* 127 (1999) 2741–2758.
- [55] R. A. Edson, J. E. Bunder, T. W. Mattner, A. J. Roberts, Lyapunov exponents of the Kuramoto–Sivashinsky PDE, *The ANZIAM Journal* 61 (2019) 270–285.
- [56] J. C. Sprott, *Elegant chaos: algebraically simple chaotic flows*, World Scientific, 2010.
- [57] P. Manneville, Liapounov exponents for the Kuramoto–Sivashinsky model, in: *Macroscopic Modelling of Turbulent Flows*, Springer, 1985, pp. 319–326.
- [58] M. Khodkar, P. Hassanzadeh, A data-driven, physics-informed framework for forecasting the spatiotemporal evolution of chaotic dynamics with nonlinearities modeled as exogenous forcings, *Journal of Computational Physics* 440 (2021) 110412.
- [59] A.-K. Kassam, L. N. Trefethen, Fourth-order time-stepping for stiff PDEs, *SIAM Journal on Scientific Computing* 2 (2005) 1214–1233.
- [60] C. M. Bishop, Pattern recognition, *Machine learning* 128 (2006).
- [61] P. A. K. Reinbold, L. M. Kageorge, M. F. Schatz, R. O. Grigoriev, Robust learning from noisy, incomplete, high-dimensional experimental data via physically constrained symbolic regression, *Nature Communications* 12 (2021) 3219.
- [62] H. Vaddirreddy, A. Rasheed, A. E. Staples, O. San, Feature engineering and symbolic regression methods for detecting hidden physics from sparse sensor observation data, *Physics of Fluids* 32 (2020).
- [63] R. Mojjani, M. Balajewicz, Stabilization of linear time-varying reduced-order models: A feedback controller approach, *International Journal for Numerical Methods in Engineering* 121 (2020) 5490–5510.